Electronic supplementary information

Novel High Performance Asymmetrical Squaraines for Small Molecule Organic Solar Cells with a High Open Circuit Voltage of 1.12 V

Daobin Yang,[a]‡ Qianqian Yang,[b]‡ Lin Yang,[a] Qian Luo,[a] Yan Huang,*[a] Zhiyun Lu*[a] and Suling Zhao*[b]

[a] *Key Laboratory of Green Chemistry and Technology (Ministry of Education), College of Chemistry, Sichuan University, Chengdu 610064, P. R. China. E-mail: huangyan@scu.edu.cn (Y. Huang); luzhiyun@scu. edu.cn (Z. Lu);*

[b] *Key Laboratory of Luminescence and Optical Information (Ministry of Education), Institute of Optoelectronics Technology, Beijing Jiaotong University, Beijing 100044, P. R. China. E-mail: slzhao@ bjtu.edu.cn (S. Zhao)*

‡ The first two authors contributed equally to this work.

Table of contents

Experimental details

Instruments and characterization

^{1}H NMR and ^{13}C NMR spectra were measured using a Bruker Avance AV II-400 MHz spectrometer, and the chemical shifts were recorded in units of ppm with TMS as the internal standard. FT-IR spectra were recorded on a Perkin-Elmer 2000 infrared spectrometer with KBr pellets under an ambient atmosphere. Single crystal X-ray diffraction data of the target molecules were obtained on a Xcalibur E X-ray single crystal diffractometer equipped with graphite monochromator Mo-Ka (λ= 0.71073 Å) radiation. The data collection was executed using CrysAlisPro program. The structures were determined using direct method and successive Fourier difference syntheses (SHELXS-97) and refined using full-matrix leastsquares procedure on F2 with anisotropic thermal parameters for all non-hydrogen atoms (SHELXL-97). Single crystal X-ray structures were obtained for a metallic yellow crystals of ASQB obtained from CH_2Cl_2/CH_3OH (CCDC number: 925658) and ASQC obtained from $CHCl_3/CH_3OH$ (CCDC number: 944996). The ground-state geometries and electronic structures of ASQB and ASQC were calculated with Gaussian 03 software, using density functional theory (DFT) based on B3LYP/ 6-31G level.

Electronic absorption spectra of both solution and thin-film of the small molecules were recorded using a Hitachi U-4100 UV-Vis-NIR scanning spectrophotometer. The solution samples were prepared in chloroform solution at a concentration of 5.23×10^{-6} mol L^{-1} of ASQB and 5.67×10^{-6} mol L^{-1} of ASQC, while the film samples were obtained by spin-coating from chloroform solution (5 mg mL^{-1}, 1000 rpm/ 40 s) on quartz substrates. Cyclic voltammetry measurements were carried out in 2.5×10^{-4} mol L^{-1} anhydrous acetonitrile with tetrabutylammonium hexafluorophosphate (Bu_4NPF_6) under an argon atmosphere at a scan rate of 50 mV s^{-1} using a LK 2005A electrochemical workstation. The CV system was constructed using a Pt disk, a Pt wire, and a $Ag/AgNO_3$ (0.1 mol L^{-1} in acetonitrile) electrode as the working electrode, counter electrode and reference electrode, respectively, and the potential of the

$Ag/AgNO_3$ reference electrode was internally calibrated using the ferrocene/ ferrocenium redox couple (Fc/ Fc^+), which has a known reduction potential of -4.80 eV relative to vacuum level. The morphologies of the active layers were analyzed through atomic force microscopy (AFM) in tapping mode under ambient conditions using a MFP 3D Asylum Research instrument.

Fabrication and characterization of organic solar cells devices

Small molecules bulk-heterojunction organic solar cells were fabricated using indium-tin-oxide (ITO) coated glass as substrate. The thickness of ITO is 190 nm and sheet resistance is 15 Ω/sq. The substrate was cleaned consecutively in ultrasonic baths containing detergent, deionized water, acetone and ethanol for 10 min each, and finally blow-dried by high purity nitrogen. The substrate was treated by UV-ozone for 5 min, then immediately transferred into a high vacuum chamber for deposition of 80 Å MoO_3 at pressures of less than 3×10^{-4} Pa with a rate of 0.5 Å s^{-1}. Subsequently, photoactive layers were fabricated by spin-coating a blend of the target molecules and $PC_{71}BM$ in chloroform with total concentration of 20 mg mL^{-1} (1500 rpm, 30 s) under a N_2-filling glovebox at 25 °C. The solution mixtures were stirred for 12 h at room temperature. Then the substrates were loaded into a vacuum chamber to finish the deposit LiF (8 Å) and Al (1000 Å) at pressures of less than 3×10^{-4} Pa with a rate of 0.05 Å s^{-1} and 1.5 Å s^{-1}, respectively. Deposition rate and film thickness were in situ monitored using a quartz crystal oscillator mounted to the substrate holder. The active area of OPV cells is 6 mm^2. The current-voltage curves under illumination were measured using an Abet solar simulator with a Keithley 4200 source measurement unit under AM 1.5G illumination (100 mW/cm^2), after spectral mismatch correction under an ambient atmosphere at 25 °C. Hole-only devices were fabricated with the structure of ITO/ MoO_3 (8 nm)/ASQ: $PC_{71}BM$ (80 nm)/Au (100 nm). The EQE measurements were performed in air using a QE/IPCE Measurements Solar Cell Scan 100 (ZOLIX) system.

Synthesis

5-*N,N*-Diisobutylamino-1,3-dihydroxybenzene (**2a**) [1] was prepared according to the procedures described in the literature. n-Butanol and toluene were distilled from sodium freshly prior to use. All other chemicals were obtained from commercial sources and used as-received without further purification.

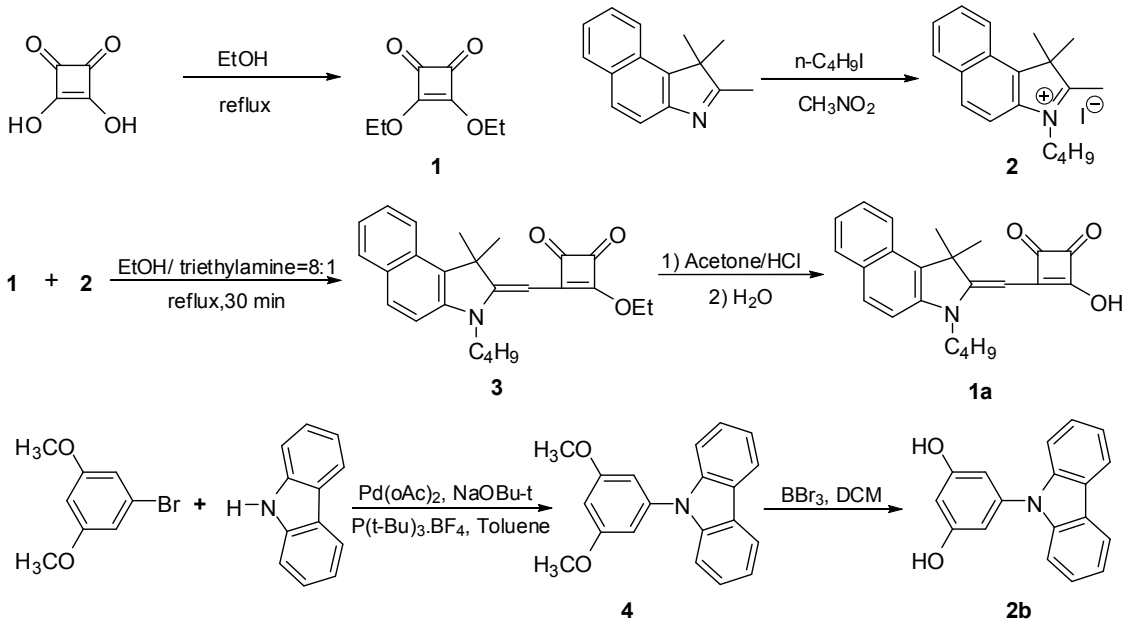

Scheme 1. Synthetic routes to the intermediates.

3,4-Diethoxy-cyclobut-3-ene-1,2-dione (1) [2]

squaric acid (5.00 g, 43.8 mmol) was suspended in 50 mL anhydrous ethanol and refluxed for 2 h. After 30 min the squaric acid was dissolved and the ethanol was removed under vacuum. Then, 50 mL of anhydrous ethanol was added, the mixture was refluxed for 1 h and the solvent was removed again. This step was repeated three times. After removement of solvent, the crude product was purified by silica gel chromatography (eluent, hexane/ethyl acetate= 6:1) to afford compound **1** as a light yellow oil (6.11 g, 82%). ^{1}H NMR (400 MHz, $CDCl_3$, ppm) δ: 4.77 (4H, q, *J*=7.0 Hz, -OCH_2-), 1.50 (6H, t, *J*=7.0 Hz, -CH_3).

3-Butyl-1,1,2-trimethyl-1H-benzo[e]indolium Iodide (2) [3]

1,1,2-Trimethyl-1*H*-benzo[e]indole (5.00 g, 23.9 mmol), and nitromethane (80 mL)

were mixed in a round bottom flask. After the material was dissolved, iodobutane (8.80 g, 47.8 mmol) was added dropwise slowly at room temperature and the reaction mixture was magnetically stirred for 12 h. Another portion of iodobutane (2.20 g, 11.9 mmol) was added, then heated at 80 °C for 12 h. The cooled reaction mixture was triturated with diethyl ether (400 mL) and the precipitate was filtered off, washed with diethyl ether three times, and dried in vacuum to obtain compound **2** as a pale-green crystal (7.80 g, 83%), mp 165-168 °C.

3-Ethoxy-4-((3-butyl-1,1-dimethyl-1H-benzo[e]indol-2(3H)-ylidene)methyl)cyclobut-3-ene-1,2-dione (3)

Compound **2** (5.00 g, 12.7 mmol), anhydrous ethanol (200 mL) and triethylamine (25 mL) were added into a three neck round bottom flask and refluxed for 30 min. After the Compound **2** was dissolved, the solution was cooled to room temperature. Compound **1** (1.80 g, 10.6 mmol) was added dropwise slowly. Then, the reaction mixture was heated at 60 °C for 4 h and the solvent was evaporated under reduced pressure, the residue was recrystallized from anhydrous ethanol three times to afford compound **3** as a yellow crystal (3.20 g, 78%), mp 187-188 °C (from ethanol). ^{1}H NMR (400MHz, $CDCl_3$, ppm) δ: 8.11 (1H, d, *J*=8.4 Hz, Ar), 7.89 (1H, d, *J*=8.4 Hz, Ar), 7.85 (1H, d, *J*=8.4 Hz, Ar), 7.56 (1H, t, *J*=7.6 Hz, Ar), 7.40 (1H, t, *J*=7.6 Hz, Ar), 7.23 (1H, d, *J*=8.8 Hz, Ar), 5.46 (1H, s, =CH-), 4.96 (2H, q, *J*=7.2 Hz, -CH_2-), 3.96 (2H, t, *J*=7.2 Hz, -NCH_2-), 1.90 (6H, s, -CH_3), 1.83-1.76 (2H, m, -CH_2-), 1.58 (3H, t, *J*=7.0 Hz, -CH_3), 1.50-1.43 (2H, m, -CH_2-), 1.03 (3H, t, *J*=7.2 Hz, -CH_3).

3-((3-Butyl-1,1-dimethyl-1H-benzo[e]indol-2(3H)-ylidene)methyl)-4-hydroxycyclobut-3-ene-1,2-dione (1a)

Compound **3** (1.24 g, 3.18 mmol) were dissolved in 40 mL acetone and refluxed. After the Compound **3** was dissolved, 15 mL of a 6 M HCl solution was added dropwise and heated for 90 min. After that, 50 mL deionized water was dropped to the reaction mixture which precipitated the yellow solid. The resulted mixture is filtered and the product was washed by deionized water to afford bright yellow powder

compound **1a** (1.00 g, 87 %), dp. 198 °C. ^{1}H NMR (400MHz, DMSO-d_6, ppm) δ: 8.07 (1H, d, *J*=8.8 Hz, Ar), 7.86 (1H, d, *J*=8.0 Hz, Ar), 7.82 (1H, d, *J*=8.8 Hz, Ar), 7.47 (1H, t, *J*=7.6 Hz, Ar), 7.36 (1H, d, *J*=8.8 Hz, Ar), 7.25 (1H, t, *J*=7.6 Hz, Ar), 5.45 (1H, s, =CH-), 3.85 (2H, t, *J*=7.2 Hz, -NCH_2-), 1.83 (6H, s, -CH_3), 1.66-1.61 (2H, m, -CH_2-), 1.42-1.36 (2H, m, -CH_2-), 0.95 (3H, t, *J*=7.2 Hz, -CH_3).

5-*N*-carbazolyl-1,3-dimethoxybenzene (4) [4]

A mixture of carbazole (5.00 g, 29.9 mmol), 1-bromo-3,5-dimethoxybenzene (7.80 g, 35.9 mmol), NaOBu-*t*[Sodium tert-butoxide](5.74 g, 59.8 mmol), $Pd(OAc)_2$ [Palladium (II) acetate] (134 mg, 2%), and P(*t*-Bu)$_3$ BF_4 [Tri-tert-butylphosphine tetrafluoroborate] (347 mg, 4%) were dissolved in 200 mL of toluene and refluxed under Ar for 10 h. The reaction mixture was cooled down and passed through a filter paper to remove insoluble material, then the solvents were removed under reduced pressure. The crude product was purified by silica gel chromatography (eluent, hexane/ethyl acetate= 15:1) to afford compound **4** as a white solid (6.60 g, 73%), mp 76-77 °C. ^{1}H NMR (400 MHz, $CDCl_3$, ppm) δ: 8.15 (2H, d, *J*=8.0 Hz, Ar), 7.50 (2H, d, *J*=8.0 Hz, Ar)，7.44 (2H, t, *J*=7.8 Hz, Ar), 7.30 (2H, t, *J*=7.8 Hz, Ar), 6.72 (2H, s, Ar), 6.57 (1H, s, Ar), 3.84 (6H, s, -OCH_3).

5-*N*-carbazolyl-1,3-dihydroxybenzene (2b) [4]

Compound **4** (1.50 g, 4.95 mmol) was added to 60 mL of anhydrous CH_2Cl_2. Boron tribromide (50 mL of 1 M solution in CH_2Cl_2, 49.5 mmol) was added dropwise slowly at ice bath, then the solution was stirred under room temperature for 24 h. The solution was then decanted to 100 mL of ice water to remove any excess of BBr_3, the organic phase was separated, and the aqueous phase was extracted with CH_2Cl_2 for three times. The combined organic phases were washed with saturation aqueous $NaHCO_3$ solution and water, dried over anhydrous Na_2SO_4. After removing solvent under vacuum, a white solid compound **2b** (1.30 g, 95%) was obtained. ^{1}H NMR ($CDCl_3$, 400 MHz, ppm) δ: 8.13 (2H, d, *J*=8.0 Hz, Ar), 7.50 (2H, d, *J*=8.0 Hz, Ar), 7.43 (2H, t, *J*=7.2, 8.0 Hz, Ar), 7.30 (2H, t, *J*=7.2 Hz, Ar), 6.63 (2H, s, Ar), 6.45 (1H, s, Ar).

2-[(3-Butyl-1,1-dimethyl-1H-benzo[e]indol-2(3H)-ylidene)methyl]-4-[(4-(*N*,*N*-diiso-butylamino)-2,6-dihydroxyphenyl)-2,5-dien-1-ylidene]-3-oxocyclobut-1-en-1-olate (ASQB)

A mixture of compound **1a** (2.00 g, 5.53 mmol) and **2a** (1.32 g, 5.53 mmol) in n-butanol (100 mL) and toluene (100 mL) were added into a round bottom flask. The mixture was refluxed with a Dean-Stark apparatus for 24 h. After reaction was cooled down, the solvents were removed under reduced pressure. The crude product was purified by silica gel chromatography using dichloromethane/ methanol (50:1, v/v) as the eluent to afford brown solid. The solid was recrystallized from a 1:4 volume ratio of dichloromethane and methanol mixture to afford golden crystals with metallic lustre of **ASQB** (0.92 g, 29%), mp 198-199 °C. FI-IR: ν_{max}/cm^{-1} 2956, 2868, 1636 (C-O), 1557, 1403, 1321, 1249, 1197, 1119, 932, 803; ^{1}H NMR (400 MHz, $CDCl_3$, ppm) δ:12.41 (2H, s, -OH), 8.21 (1H, d, *J*=8.4 Hz, Ar), 7.93 (1H, d, *J*=7.6 Hz, Ar), 7.91 (1H, d, *J*=8.4 Hz, Ar), 7.61 (1H, t, *J*=7.6 Hz, Ar), 7.48 (1H, t, *J*=7.6 Hz, Ar), 7.33 (1H, d, *J*=8.8 Hz, Ar), 5.85 (1H, s, =CH-), 5.80 (2H, s, Ar), 4.15 (2H, t, *J*=7.4 Hz, -NCH_2-), 3.23 (4H, d, *J*=7.6 Hz, -CH_2-), 2.20-2.10 (2H, m, -CH_2-), 2.01 (6H, s, -CH_3), 1.88-1.81 (2H, m, -CH_2-), 1.54-1.44 (2H, m, -CH_2-), 1.03 (3H, t, *J*=7.4 Hz, -CH_3), 0.93 (12H, d, *J*=6.8 Hz, -CH_3); ^{13}C NMR (100 MHz, $CDCl_3$, ppm) δ: 173.46, 170.20, 166.72, 163.13, 157.41, 139.19, 135.09, 131.71, 130.10, 129.88, 128.52, 127.67, 124.99, 122.72, 110.38, 102.96, 93.79, 86.39 (Ar), 60.38, 51.63, 44.09, 29.67, 27.63, 26.68, 20.43, 20.32, 13.97 (alkyl). ESI-MS: *m/z* 581.22 [M^+].

2-[(3-Butyl-1,1-dimethyl-1H-benzo[e]indol-2(3H)-ylidene)methyl]-4-[(4-(*N*-carbaz olyl)-2,6-dihydroxyphenyl)-2,5-dien-1-ylidene]-3-oxocyclobut-1-en-1-olate (ASQC)

A mixture of compound **1a** (1.03 g, 2.85 mmol) and compound **2b** (0.94 g, 3.42 mmol) in n-butanol (30 mL) and toluene (90 mL) were added into a round bottom flask. The mixture was refluxed with a Dean-Stark apparatus for 24 h. After reaction was cooled down, the solvents were removed under reduced pressure. The crude product was purified by silica gel chromatography using hexane/ethyl acetate(3:1, v/v) as the eluent to afford brown solid. The solid was recrystallized from a 1:4 volume ratio of

dichloromethane and methanol mixture to afford golden crystals with metallic lustre of **ASQC** (0.21 g, 13%), mp 222-223 °C. FI-IR: ν_{max}/cm^{-1} 2955, 2924, 1634 (C-O), 1562, 1418, 1324, 1301, 1200, 1117, 933, 803, 748; ^{1}H NMR (DMSO-*d6*, 400MHz, ppm) δ: 12.20 (2H, s, -OH), 8.46 (1H, d, *J*=8.4 Hz, Ar), 8.24 (2H, d, *J*=7.6 Hz, Ar), 8.23 (1H, d, *J*=9.2 Hz, Ar), 8.19 (1H, d, *J*=8.0 Hz, Ar), 8.09 (1H, d, *J*=9.2 Hz, Ar), 7.78 (1H, t, *J*=7.2 Hz, Ar), 7.69 (1H, t, *J*=7.2 Hz, Ar), 7.61 (2H, d, *J*=8.4 Hz, Ar), 7.50 (2H, t, *J*=7.2 Hz, Ar), 7.34 (2H, t, *J*=7.2 Hz, Ar), 6.55 (2H, s, Ar), 6.43 (1H, s, =CH-), 4.66 (2H, t, *J*=7.2 Hz, -NCH$_2$-), 2.02 (6H, s, -CH$_3$), 1.91-1.83 (2H, m, -CH$_2$-), 1.52-1.43 (2H, m, -CH$_2$-), 0.99 (3H, t, *J*=7.2 Hz, -CH$_3$); ^{13}C NMR (100 MHz, CDCl$_3$, ppm) δ: 184.10, 181.08, 178.85, 174.45, 166.35, 162.04, 161.54, 145.29, 139.78, 137.94, 137.70, 132.78, 130.83, 129.96, 128.3,1 127.99, 126.58, 126.07, 124.00, 122.96, 120.48, 120.17, 111.17, 110.75, 108.03, 106.20, 106.05, 90.04 (Ar), 53.35, 45.50, 30.17, 25.94, 20.26, 13.76 (alkyl). ESI-MS: *m/z* 619.30 [M^{+}].

Table S1 Solubility of the small molecule in different solvents at 15 °C (mg mL^{-1})

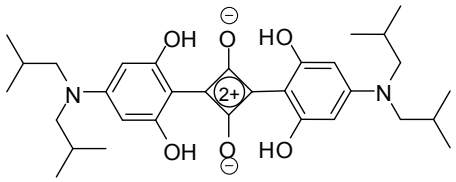

DPSQ [5]

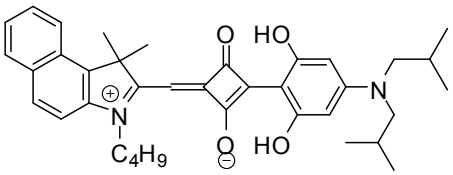

ASQB

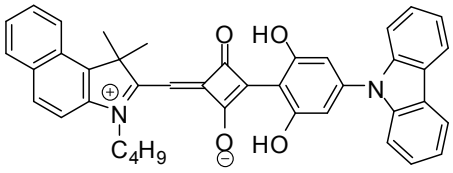

ASQC

Solvent	HX	TU	CF	CB	DCB	AT	THF	MeOH
DPSQ	---	< 1	< 6	< 2	< 2	< 1	< 0.7	---
ASQB	< 0.1	> 30	> 90	> 90	> 90	> 50	> 20	< 0.1
ASQC	---	> 25	> 80	> 80	> 80	> 25	> 40	< 0.1

Note: HX=Hexane, TU=toluene, CF=chloroform, CB=chlorobenzene, DCB=1,2- dichlorobenzene, AT=acetone, THF=tetrahydrofuran, MeOH=methanol, ---= insoluble

Table S2 Summary of crystal data, data collection and refinement parameters for (ASQB CCDC number: 925658, ASQC CCDC number: 944996 and DPSQ [5])

Compound	**ASQB**	**ASQC**	**DPSQ**
Empirical formula	$C_{38}H_{48}N_2O_5$	$C_{42}H_{38}N_2O_5$	$C_{32}H_{44}N_2O_6$
Formula weight	612.78	650.74	552.69
Temperature	143.05 K	140.15 K	143(2)K
Crystal system	monoclinic	orthorhombic	monoclinic
Space group	$P2_1/c$	Pbca	P2(1)/n
a/Å	14.5029(4)	19.297(2)	6.2034(16)
b/Å	16.1542(5)	14.3767(17)	16.478(4)
c/Å	15.0028(5)	24.546(3)	14.518(4)
α/°	90.00	90.00	90
β/°	107.744(3)	90.00	92.406
γ/°	90.00	90.00	90
Volume/$Å^3$	3347.68(18)	6809.7(14)	1482.7(6)
Z	4	8	2
$\rho_{calc}mg/mm^3$	1.216	1.269	1.238
m/mm^{-1}	0.080	0.083	0.085
F(000)	1320.0	2752.0	596
Crystal size/mm^3	0.16 × 0.15 × 0.15	0.32 × 0.20 × 0.03	0.33× 0.09 × 0.05
2θ range for data collection	5.8 to 52.74°	3.32 to 62.14°	1.87 to 27.52°
Index ranges	-14 ≤ h ≤ 18, -20 ≤ k ≤ 15, -18 ≤ l ≤ 15	-27≤ h ≤ 26, -19 ≤ k ≤ 20, -35 ≤ l ≤ 35	-8≤ h ≤ 8, -21 ≤ k ≤ 20, -18 ≤ l ≤ 18
Reflections collected	14519	65056	12527
Independent reflections	6829 [R(int) = 0.0316]	10416 [R(int) = 0.0903]	3349 [R(int) = 0.0508]
Data/restraints/parameters	6829/0/417	10416/0/449	3349/0/193
Goodness-of-fit on F^2	1.015	0.983	1.014
Final R indexes [I>=2σ (I)]	R_1 = 0.0540, wR_2 = 0.1016	R_1 = 0.0516, wR_2 = 0.1304	R_1 = 0.0477, wR_2 = 0.1021
Final R indexes [all data]	R_1 = 0.0937, wR_2 = 0.1183	R_1 = 0.1119, wR_2 = 0.1664	R_1 = 0.0890, wR_2 = 0.1147
Largest diff.peak/hole/e $Å^{-3}$	0.28/-0.21	0.31/-0.23	0.218/-0.184

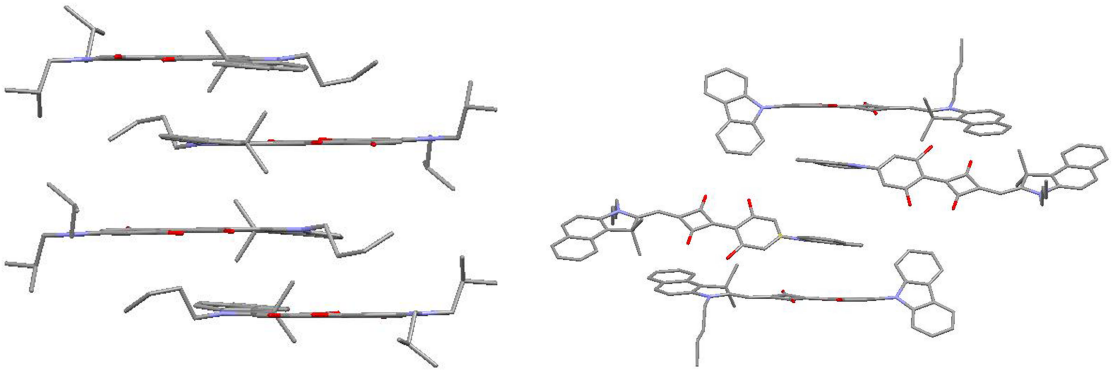

Fig. S1 Crystal packing diagrams for ASQB (left) and ASQC (right).

DPSQ Crystal Data

The dihedral angle between the squarate core and phenyl moiety in DPSQ (dihedral angle 3.52°) is smaller than the ASQs (ASQB and ASQC), which is may due to the existence of four strong hydrogen bonding interactions (O···H-O). According to the packing diagrams of the compound DPSQ (Fig. S2), the shortest distance between two neighboring is 3.75 Å.

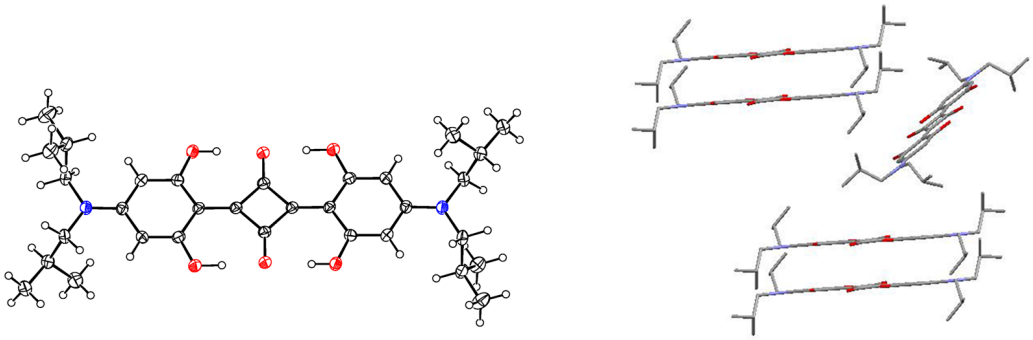

Fig. S2 ORTEP diagrams (left) and crystal packing diagrams (right) for DPSQ [5].

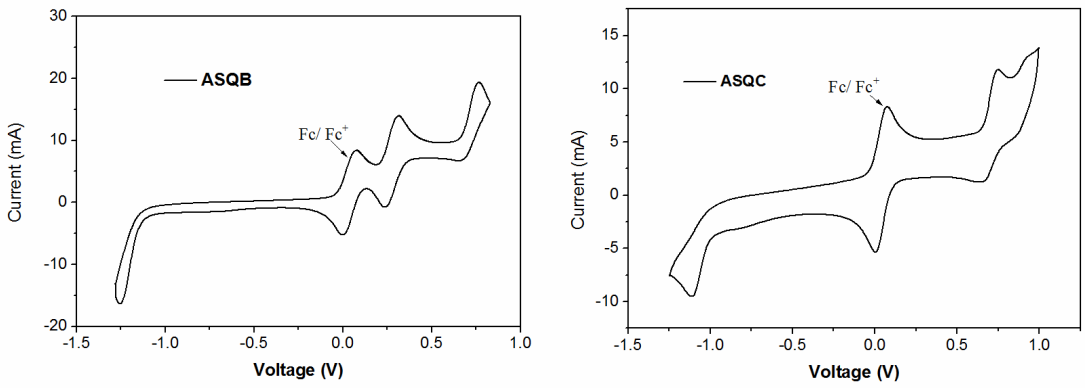

Fig. S3 Cyclic voltammogram of the target compounds in acetonitrile solution.

Table S3 The photovoltaic performances of the organic solar cells based on ASQC: $PC_{71}BM$ blends with different weight ratios.

Active layer (w/ w)	V_{oc} (V)	J_{sc} (mA cm^{-2})	FF	PCE (%)
ASQC : $PC_{71}BM$ =1 : 2	1.11	4.16	0.29	1.34
ASQC : $PC_{71}BM$ =1 : 4	1.11	4.78	0.32	1.70
ASQC : $PC_{71}BM$ =1 : 5	1.12	5.81	0.36	2.34
ASQC : $PC_{71}BM$ =1 : 6	1.10	4.84	0.32	1.70
ASQC : $PC_{71}BM$ =1 : 7	1.12	4.78	0.31	1.66
ASQC : $PC_{71}BM$ =1 : 10	1.12	4.05	0.29	1.32
ASQC : $PC_{71}BM$ =1 : 15	1.12	1.99	0.27	0.60
ASQC : $PC_{71}BM$ =1 : 5 [a]	1.06	7.00	0.38	2.82

a. thermo-annealing at 110 °C for 10 min.

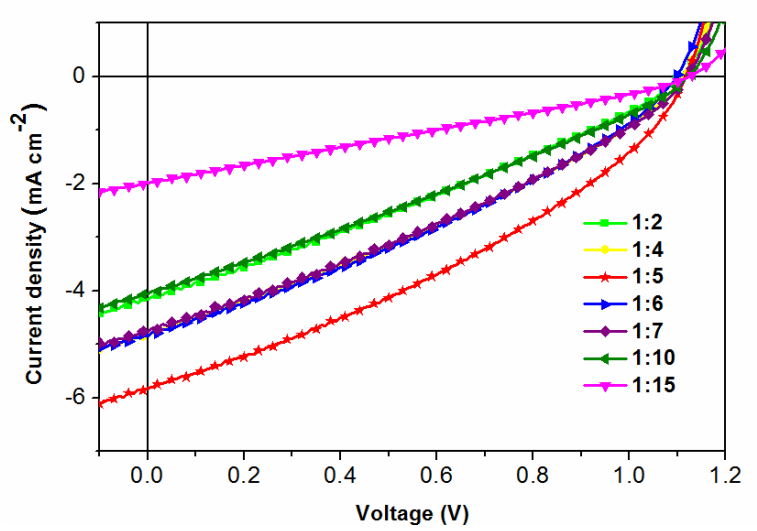

Fig. S4 *J-V* curve of the devices based on ASQC: $PC_{71}BM$ blends with different weight ratios.

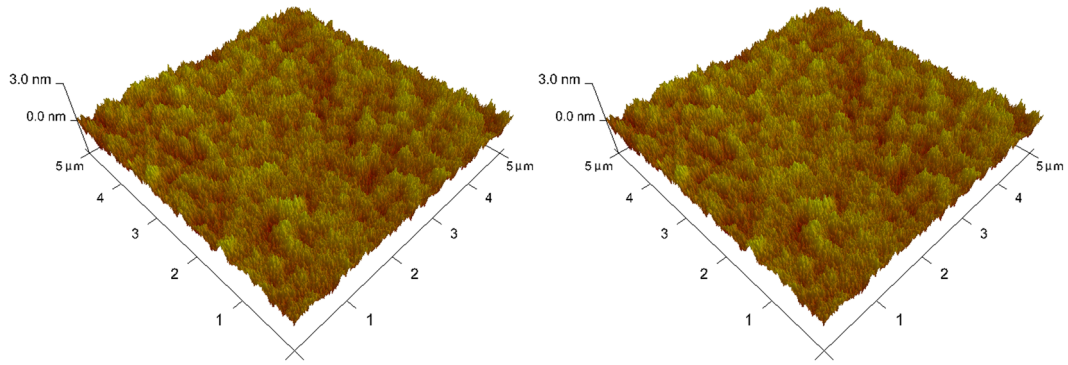

Fig. S5 3D image obtained by tapping-mode AFM showing the morphology of ASQB:$PC_{71}BM$ (1:5) blend film (size 5 × 5 μm) for root-mean-square (RMS) roughness is 0.52 nm (left) and ASQC:$PC_{71}BM$ (1:5) blend film, RMS roughness is 0.38 nm (right).

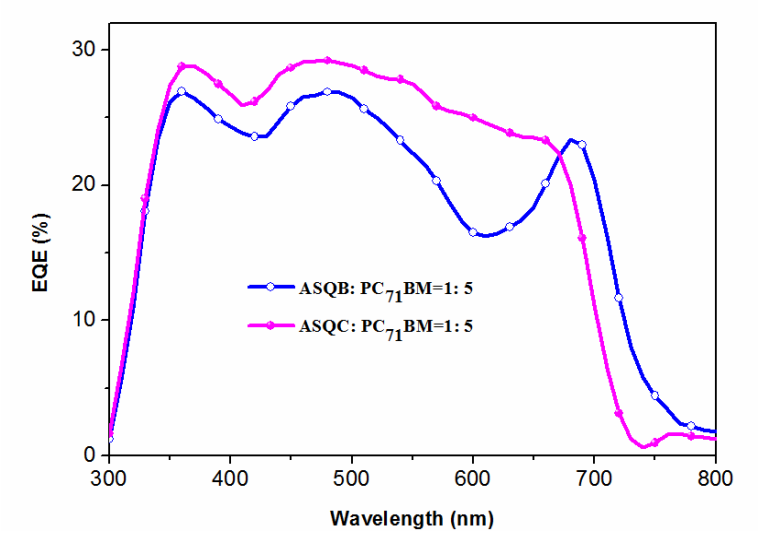

Fig. S6 EQE curves of OSC based on ASQB and ASQC devices.

Charge carrier mobilities

The hole mobility of ASQB/$PC_{71}BM$ and ASQC/$PC_{71}BM$ blend films were measured by the space charge limited current (SCLC) method with the hole-only device structure of ITO/MoO_3 (80 Å)/ASQs:$PC_{71}BM$/Au. We plot the *J-V* characterisitcs of a hole-only device, with the top cathode biased positive with respect to the anode . The data follow $J \propto V^2$, and hence are fit to a trap-free space charge limited model to extract the zero-field hole mobility, as shown in Fig. S7.

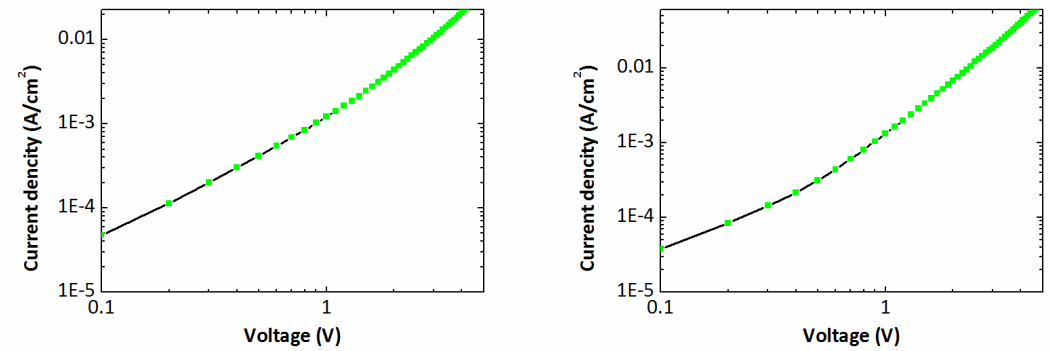

Fig. S7 *J-V* characteristic of ASQB:$PC_{71}BM$ (1:5) (left) and ASQC:$PC_{71}BM$ (1:5) (right) single carrier devices used for hole mobility measurement.

References

[1] M. Q. Tian, M. Furuki, I. Iwasa, Y. Sato, L. S. Pu and S. Tatsuura, *J. Phys. Chem. B*, 2002, **106**, 4370.

[2] J. H. Yum, P. Walter, S. Huber, D. Rentsch, T. Geiger, F. Nüesch, F. De Angelis, M. Grätzel and M. K. Nazeeruddin, *J. Am. Chem. Soc.,* 2007, **129**, 10320.

[3] M. V. Kvach, A. V. Ustinov, I. A. Stepanova, A. D. Malakhov, M. V. Skorobogatyi, V. V. Shmanai and V. A. Korshun, *Eur. J. Org. Chem.*, 2008, **2008**, 2107.

[4] *US Pat*., 7 851 579, 2010.

[5] S. Wang, L. Hall, V. V. Diev, R. Haiges, G. Wei, X. Xiao, P. I. Djurovich, S. R. Forrest and M. E. Thompson, *Chem. Mater.*, 2011, **23**, 4789